



Research article

UDC 693.5


DOI: 10.34910/MCE.124.4



Planting steel reinforcement for concrete columns

M.M. Kharnoob 

University of Baghdad, Baghdad, Iraq

 dr.majidkharnoob@coeng.uobaghdad.edu.iq

Keywords: column, implantation, pull-out, steel fiber, bond, slip

Abstract. This study presents a scenario where the embedding of dowel reinforcement for new columns was inadvertently omitted during the casting of concrete columns. This oversight necessitated the implantation of steel reinforcement into pre-existing cast areas. Owing to the high density of the primary slab reinforcement, implantation was feasible only up to half the slab's thickness. By modifying the superplasticizer (SP) dosage during mixing, we achieved a consistent slump of approximately 150 mm across various concrete mixes, ensuring that both slump and slump flow remained within expected limits. The properties of these mixes, both in their fresh and hardened states, are detailed in Table 2. The sieve segregation index consistently remained below 1.3 %, indicating exceptional cohesion in all concrete mixes. In fact, no segregation was observed, with all measured segregation widths being zero. In terms of strength, the cylinder strength increased significantly with the increase in fiber volume from 0 % to 2 %. This study also examines the impact of steel reinforcement, utilizing 8 mm diameter steel bars over a 30 cm length, planted at two different angles (90 and 45 degrees). The concrete column samples were subjected to uniaxial compressive load post-implantation. Results indicate that the implantation process generally led to an increase in the initial compressive strength of the concrete samples. Specifically, specimens with 30 cm reinforcement planted at distances of 55 mm and 35 mm exhibited an average strength increase of 23 % and 17 %, respectively.

Citation: Kharnoob, M.M. Planting steel reinforcement for concrete columns: In case of small distance at missing places in concrete columns. Magazine of Civil Engineering. 2023. 124(8). Article no. 12404. DOI: 10.34910/MCE.124.4

1. Introduction

This article introduces a novel integration technique for steel reinforcement in concrete columns, handy for temporary jack support in existing reinforced concrete structures. During the casting process, the inclusion of dowel reinforcement for new columns was inadvertently omitted, leading to the necessity of implanting steel reinforcement in pre-existing cast areas. The density of the primary slab reinforcement limited implantation to only half the slab's thickness. This study investigates the effect of steel reinforcement with an 8 mm diameter and 30 cm length, planted at 0 and 45 degrees angles. Post-implantation, the concrete column samples underwent uniaxial compressive load testing. Results indicated an enhancement in the initial compressive strength of the concrete samples. Specimens with 30 cm reinforcement, planted at distances of 55 mm and 35 mm, showed average strength increases of 23 % and 17 %, respectively [1–3].

Conventional reinforcement techniques include fiber-reinforced polymer (FRP) wrapping, steel cage addition, and concrete jacketing, with the latter being among the earliest and most effective methods. A recent advancement involves the application of high-performance fiber-reinforced cementitious composites (HPFRC) spray mortars with extra reinforcing bars [4]. This method demonstrated increased absorbed energy and improved cyclic response in column samples reinforced with HPFRC [5–6]. Further studies have shown that fiber-reinforced concrete significantly reduces fracture width and enhances energy

absorption. Concrete jacketing is also recognized as an effective method for restoring axial and lateral load capacities of damaged columns, though it may impose design and architectural constraints [7–9].

Alternative techniques, like FRP sheet external confinement, have gained attention. Research on FRP wrapping has highlighted its effectiveness in restoring damaged concrete columns, with reinforced columns showing increased axial load capacity [10–12]. However, the effectiveness of this strategy heavily relies on the column design.

Standard methods for curing concrete after completion include gluing for planting and planting machinery. The former involves drilling into concrete, inserting rebar, and filling the hole with adhesive, usually epoxy resin or cement [13–14]. This method is popular for its on-site applicability. Since the 1990s, cement-based materials for rebar planting have been replaced by various adhesives like polyester, vinyl ester, and epoxy. A pull-out test using two epoxies with steel models of the required 16 mm diameter indicated satisfactory performance [15–25].

It is recommended to use high-quality concrete for the monolithic construction of columns. In order to reduce their cost, it is advisable to use man-made raw materials and composite binders [26–29]. Recent studies have been carried out on the mechanical behavior and structural integrity of concrete structures using various additives, bringing new insights into innovative reinforcement techniques [30,31].

2. Methods

In this study, Ordinary Portland Cement (OPC) with a 52.5N strength rating, conforming to BS EN 197-1: 2000, was utilized for the concrete mix. The OPC exhibited a Blaine fineness of 354 m²/kg as per BS EN 196-6: 2010 standards. Both fine and coarse aggregates were derived from crushed granite rock, with the fine aggregate having a maximum size of 5 mm, and the coarse aggregate a maximum size of 10 mm. According to BS 812-2: 1995 protocols, the water absorption of the fine and coarse aggregates was determined to be 1.37 % and 1.89 %, respectively, with moisture contents measured at 0.79 % for fine aggregate and 1.04 % for coarse aggregate. To achieve the desired slump of 150 ± 25 mm in each concrete mix, a poly carboxylate-based superplasticizer (SP) was incorporated, characterized by a relative density of 1.03 and a solid mass content of 20 %. For the fiber-reinforced concrete component, hooked steel fibers branded as Dramix, 30 mm in length and classified as 3D 55/30, were employed, as depicted in Fig. 1.



Figure 1. Iron Fibres used.

Table 1 outlines the Mixtures of Plain and fiber-reinforced concrete. The volume of fiber in the concrete varied between 1 and 2 %. In contrast, the water/cement (W/C) ratio for both fiber-reinforced and plain concrete was adjusted within a range of 0.55 to 0.45. Additionally, the properties of Grade 500 high-strength ribbed steel bars, with a diameter of 12.0 mm, are detailed in the third row of Table 2. As per BS EN 10080: 2005 standards, these steel reinforcement bars feature a rib pattern with 1.05 mm rib height, 8.0 mm rib spacing, a 60° angle of inclination relative to the bar axis, and a 67° rib flank inclination angle.

For experimental purposes, a 150 mm concrete cube was cast, incorporating each reinforcing bar at a length of 30 mm. In adherence to RILEM guidelines, the bond length between the concrete and reinforcement bar was set at 50 mm, which is 4.2 times the diameter of the reinforcing bar. This bonded length of 236 mm was maintained in the middle third of the concrete cube. A 50 mm long plastic tubing was fitted around the implanted reinforcing bar to prevent bonding outside the designated area. The crevice was

sealed with clay to ensure no cement paste entered the gap between the reinforcing bar and the plastic tube.

The simple mixes and the fiber-reinforced concrete were prepared using a pan mixer. All specimens underwent a 28-day curing process in a tank of lime-saturated water at a temperature of 27 ± 3 °C, as shown in Table 1, which details the composition of the concrete mix.

Table 1. Mixtures of Plain and fiber-reinforced concrete.

Mix. Concentration	Cement (Kg/m ³)	Fine (Kg/m ³)	Water (Kg/m ³)	10 mm agg. (Kg/m ³)	Steel fibre (Kg/m ³)
0.0%	520	830	688	680	0
1.0%	523	820	819	671	70
2.0%	460	805	833	660	80

2.1. Testing program and procedure

To assess the efficacy of a friction reduction layer (comprising a PTFE film, stainless steel plate, and grease layer), three types of specimens were prepared from each concrete mix, both plain and fiber-reinforced. These specimens underwent testing with and without using a soft rubber pad or a friction reduction layer. Three distinct testing methods were employed, designated as SRNF (Soft Rubber No Friction layer), SRFR (Soft Rubber Friction Reduction layer), and NRNF (No Rubber No Friction layer). The NRNF setup did not include a friction reduction layer or a soft rubber pad. Conversely, the SRNF setup included a soft rubber pad but omitted the friction reduction layer. The SRFR method incorporated both a friction reduction layer and a soft rubber pad.

Testing was conducted on four samples from each concrete batch to establish the bond stress-slip curve and pull-out strength for each testing method and type of concrete. The average pull-out strength and its coefficient of variation were calculated based on the results of these four tests. All pull-out tests were conducted using an MTS testing apparatus with a 250 kN load capacity. Fig. 2(a) illustrates the testing device, while Fig. 2(b) depicts the test setup.

Given that the bond length was set at 50 mm, approximately 20 % of the testing machine's capacity, the expected pull-out load was estimated at 50 kN. The bond strength was calculated using a pull-out failure load testing apparatus, as per the formula:

$$\tau = F \pi d l / 268, \quad (1)$$

where τ is bond strength, d is diameter of the reinforcing bar, F is failure load

Workability of the new concrete was assessed through slump-flow and slump tests as per BS EN 12350-8: 2010 and BS EN 12350-2: 2009 standards. The slump cone was filled with fresh concrete to its brim, and upon lifting the cone, the concrete was allowed to flow and settle. The slump was measured as the decrease in height, and the slump-flow was determined by averaging the diameters of two parallel sides of the formed concrete patties. Additionally, the average width of any paste- or mortar-free strip around the concrete patties' edge was measured to ascertain the segregation width.

Cohesiveness of the fresh concrete was evaluated using a sieve segregation test as outlined in BS EN 12350-11: 2010. The concrete sample was placed in a 300 mm diameter plastic container and left undisturbed for 15 minutes. The top 2 litres of the sample were then gently poured onto a 5 mm sieve, and after two minutes of dripping, the passed-through portion was weighed. The weight of the concrete that seeped through the sieve was calculated as a percentage of the total weight dispensed onto the sieve.

The hardened concrete's strength was determined using standard cylinder compression testing as per BS EN 12390-3: 2009, except the curing temperature set at 27 ± 3 °C. Three cylinders, each with a diameter of 150 mm and height of 300 mm, were prepared from each concrete batch and tested after 28 days. The strength result was taken as the average strength of the three cylinders, calculated at 293.

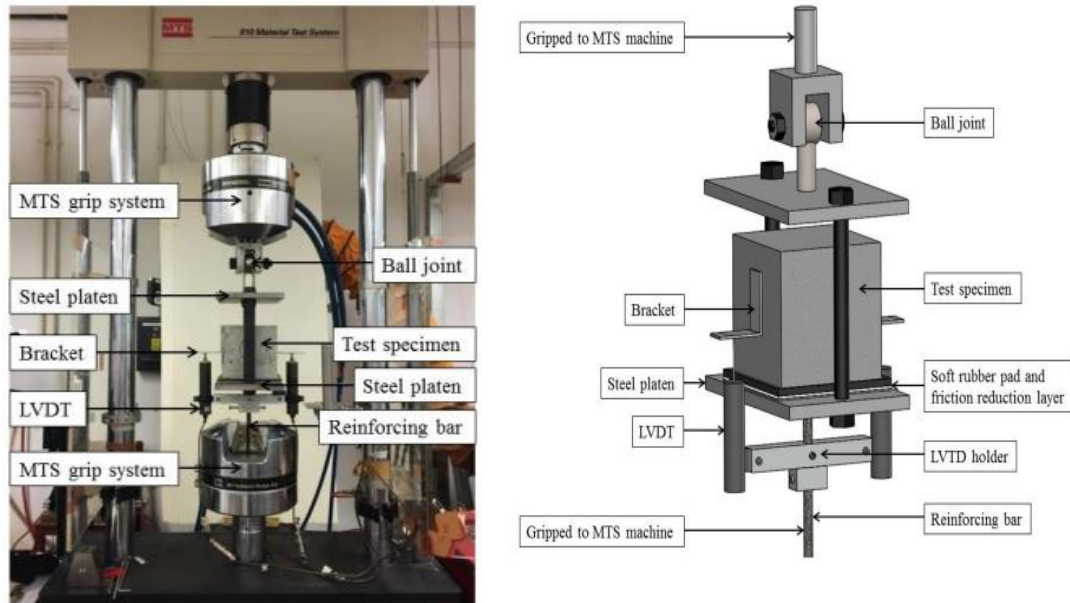


Figure 2. (a) Testing machine and test setup (b) Schematic diagram of pull out test setup.

3. Results and Discussion

3.1. Fresh and hardened Properties

During the mixing process, the superplasticizer (SP) dosage was carefully adjusted for each concrete mix, effectively achieving a target slump of approximately 150 mm. This adjustment ensured that both the slump and slump-flow values remained within the anticipated limits. The properties of these mixes, in both their fresh and hardened states, are detailed in Table 2. The sieve segregation index consistently registered below 1.3 %, indicating remarkably high cohesion across all concrete mixes, as evidenced by the cohesiveness data. Notably, actual segregation was absent in the samples, with all measured segregation widths being zero.

Regarding strength implications, a significant increase in cylinder strength was observed as the volume of fibers in the mix rose from 0 % to 2 %. This enhancement in structural integrity highlights the direct correlation between fiber volume and the compressive strength of the concrete, showcasing the efficacy of fiber reinforcement in concrete mixtures.

Table 2. The properties of the concrete mixes both Fresh and hardened.

Mix. Concentration	Slump (mm)	Slump-Flow (mm)	Cylindrical Strength (MPa)	Sieve Segregation Index (%)
0.0%	130	260	53.8	0.27
1.0%	135	240	56.4	0.15
2.0%	138	217	58.6	0.46

3.2. Bond stress-slip curves

Figure 3 displays the bond stress-slip curves for specimens with varying fiber volumes of 0.0 %, 1.0 %, and 2.0 %. Within this figure, sub-Fig. 3(a) illustrates the curve for specimens with a water/cement (W/C) ratio of 0.45, while sub-Fig. 3(b) presents the curve for those with a W/C ratio of 0.55. In each graph, a total of twelve curves are plotted, providing a comprehensive view of the bond stress-slip behavior across different fiber volumes and W/C ratios.

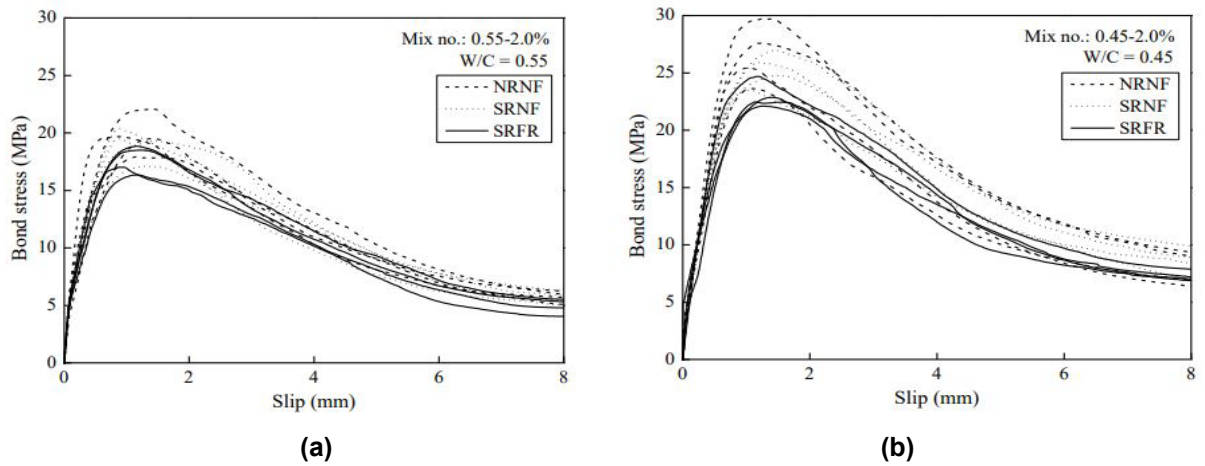


Figure 3. Bond stress-slip curves at fiber volume is 2.0 %.

Each of the twelve graphs in Fig. 3 encompasses three sets of curves corresponding to the three different test techniques (NRNF and SRNF) used for evaluating the four specimens. These curves illustrate the bond stiffness and strength derived from the bond stress-slip relationship. The specific values obtained from these curves are documented in Table 3. The subsequent section of this study delves into a detailed examination of these calculated bond stiffness and strength parameters.

Table 3. Characteristics of fresh and hardened properties of concrete mixes

Mix. Concentration	Test Technique	Individual bond Strength (MPa)			Mean of bond Strength (MPa)	Over-estimation	C.V. (%)
0.0%	SRNF	17.18	21.37	18.48	18.95	20.22	9.5
	NRNF	21.41	19.68	16.18	17.96	17.50	9.8
1.0%	SRNF	16.18	24.37	13.48	19.90	18.22	7.5
	NRNF	20.41	22.68	15.18	20.17	14.50	10.8
2.0%	SRNF	19.18	21.37	18.48	18.95	18.22	9.5
	NRNF	22.40	19.68	18.18	16.96	19.50	9.8

3.3. Mean and coefficient of variation of measured bond strength

The average bond strength can be determined by calculating the mean of four individual bond strength values obtained through a specific test procedure, as detailed in the seventh column of Table 3. Fig. 4 presents a graph illustrating the relationship between the mean calculated bond strength and the test technique, shedding light on the impact of the testing method on the measured bond strength. It was observed that the mean bond strength tended to decrease when transitioning from the NRNF to the SRNF testing technique. This decrease was expected due to the removal of the friction reduction layer and soft rubber pad from the interface between the concrete block and steel plate, which diminishes the confining stresses and consequently lowers the observed bond strength by allowing greater lateral expansion of the concrete. The SRFR method, combining a soft rubber pad with a friction reduction layer, yielded the lowest bond strength, likely offering a more accurate representation of the inherent bond strength. Other methods that exclude either the friction-reducing layer or the soft rubber pad tend to overestimate the bond strength.

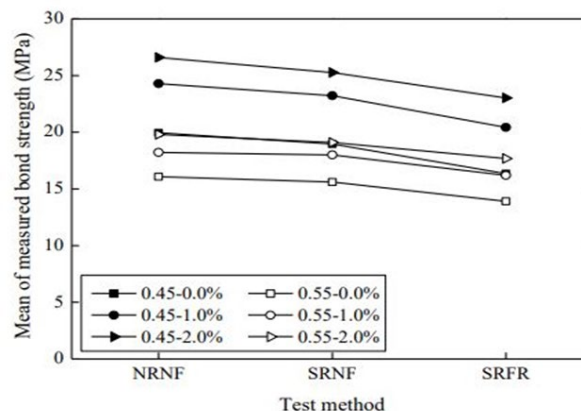


Figure 4. The effect of test procedure on the mean of measured bond strength.

The percentage overestimation of bond strength when using the NRNF method compared to the SRNF is documented in the eighth column of Table 3. These results show that the NRNF method overestimated bond strength by approximately 12.0 % to 22.0 %, whereas the SRNF method overestimated it by about 8.0 % to 16.0 %. This overestimation was more pronounced at lower W/C ratios and smaller fiber volumes. In scenarios lacking both a soft rubber pad and a friction reduction layer, the error in bond strength measurement could reach 20 %; however, with only a soft rubber pad present, the error could still be as high as 15 %. These findings highlight the necessity for improved test setups, especially at lower W/C ratios where inaccuracies in bond strength measurements could be more severe, indicating the importance of a more precise test apparatus for high-strength concrete.

The impact of internal confinement from additional fibers might explain the higher bond strength values at lower fiber volumes. Introducing fibers generally reduces the Poisson's ratio and lateral expansion of the concrete due to the fibers' internal restriction against lateral expansion. This internal confinement effect of the fibers would likely diminish the external confinement impact at the interface between concrete block and steel plate. The coefficient of variation (C.V.) of bond strength using all three test methodologies was also calculated, as shown in the final column of Table 3. Fig. 4 displays a graph correlating the estimated C.V. of measured bond strength with the test methodology, indicating that the test method significantly influences the variance in observed bond strength. For instance, the C.V. ranged from approximately 8.4 % to 13.2 % for NRNF, 4.5 % to 9.1 % for SRNF, and 4.4 % to 6.8 % for SRFR. The substantial reduction in C.V. achieved by the friction reduction layer can be attributed to its ability to minimize highly variable external confinement and the soft rubber pad's capacity to mitigate random fluctuations in contact pressure at the interface between concrete block and steel plate. This reduction in C.V. enhances the reliability and repeatability of the pull-out test, which is crucial for establishing design bond strength in structural analysis and design.

4. Conclusions

Despite the significant influence of bond properties of reinforcing bars on the structural behavior of reinforced concrete structures, there is currently no universally accepted test procedure for their measurement. Existing test methods often neglect the potential effects of boundary conditions at the interface between concrete block and steel plate. Addressing this gap, a finite element analysis was conducted to examine the impact of these boundary conditions, leading to the development of a new test method incorporating a soft rubber pad and a friction reduction layer at the interface. The primary goal of this novel method is to mitigate test errors caused by friction and uneven contact pressure. To assess the effectiveness of this approach, 72 specimens, both of plain and fiber-reinforced concrete with fiber volumes up to 2 %, were examined. The key conclusions drawn are as follows:

1. The discontinuous contact pressure and friction at the interface between concrete block and steel plate can significantly influence the confining stresses on the concrete around the reinforcing bar, consequently affecting the measured bond properties.
2. Introducing a soft rubber pad at the interface markedly reduces the measured bond strength and stiffness, thereby minimizing the overestimation of these bond properties. This addition also substantially diminishes the random variations in test results, enhancing the repeatability and reliability of the pull-out test.

References

1. Terai, M., Minami, K. Fracture behavior and mechanical properties of bamboo reinforced concrete members. *Procedia Engineering*. 2011. 10. Pp. 2967–2972.
2. Dahmani, L., Khennane, A., Kaci, S. Crack identification in reinforced concrete beams using ANSYS software. *Strength of materials*. 2010. 42 (2). Pp. 232–240.
3. Abed, F., El-Chabib, H., AlHamaydeh, M. Shear characteristics of GFRP-reinforced concrete deep beams without web reinforcement. *Journal of Reinforced Plastics and Composites*. 2012. 31(16). Pp. 1063–1073.
4. Chu, S.H., Kwan, A.K.H. A new method for pull out test of reinforcing bars in plain and fibre reinforced concrete. *Engineering Structures*. 2018. 164. Pp. 82–91. DOI: 10.1016/j.engstruct.2018.02.080
5. Jing, D., Cao, S., Krevaikas, T., Bian, J. A self-locking steel bearing connection for circular reinforced concrete columns. *Advances in Structural Engineering*. 2019. 22(12). Pp. 2605–2619. DOI: 10.1177/1369433219849810
6. Mohsin, S.S., Abbas, A., Cotsovos, D. Shear behaviour of steel-fibre-reinforced-concrete beams. In 11th International Conference on Concrete Engineering and Technology. 2012. 2014. Pp. 362–368.
7. Hashemi, N., Vatani Oskouei, A., Doostmohamadi, A. A Rehabilitation Experimental Program on Low-Strength Concrete with Steel Bar Planting. *Journal of Rehabilitation in Civil Engineering*. 2021. 9(2). Pp. 85–100.
8. Faisal, B., Izzet, A.F. Post Fire Residual Concrete and Steel Reinforcement Properties. *IOP Conference Series Earth and Environmental Science*. 2021. 856(1). 012058. DOI: 10.1088/1755-1315/856/1/012058
9. Tobbi, H., Farghaly, A.S., Benmokrane, B. Concrete Columns Reinforced Longitudinally and Transversally with Glass Fiber-Reinforced Polymer Bars. *ACI Structural Journal*. 2012. 109(4). 109-S48.

10. Aboukifa, M., Moustafa, M.A. Experimental seismic behavior of ultra-high performance concrete columns with high strength steel reinforcement. *Engineering Structures*. 2021. 232. 111885.
11. Mohammed, H., Said, A. Residual strength and strengthening capacity of reinforced concrete columns subjected to fire exposure by numerical analysis. *Journal of the Mechanical Behavior of Materials*. 2022. 31(1). Pp. 212–224. DOI: 10.1515/jmbm-2022-0026
12. Zhao, B., Taucer, F., Rossetto, T. Field investigation on the performance of building structures during the 12 May 2008 Wenchuan earthquake in China. *Engineering Structures*. 2009. 31(8). Pp. 1707–1723.
13. Hedebratt, J., Silfwerbrand, J. Full-scale test of a pile supported steel fibre concrete slab. *Materials and Structures*. 2014. 47(4). Pp. 647–666. DOI: 10.1617/s11527-013-0086-5
14. Eamon, C.D., Jensen, E. Reliability analysis of prestressed concrete beams exposed to fire. *Engineering Structures*. 2012. 43. Pp. 69–77. DOI: 10.1016/j.engstruct.2012.05.016
15. Garden, H.N., Hollaway, L.C., Thorne, A.M., Robust. A preliminary evaluation of carbon fibre reinforced polymer plates for strengthening reinforced concrete members. *Proceedings of the Institution of Civil Engineers – Structures and Buildings*. 1997. 122(2). Pp. 127–142. DOI: 10.1680/istbu.1997.29302
16. Johnson, R.P. *Composite Structures of Steel and Concrete: beams, slabs, columns and frames for buildings*. John Wiley & Sons, 2018.
17. Papakonstantinou, C.G., Petrou, M.F., Harries, K.A. Fatigue behavior of RC beams strengthened with GFRP sheets. *Journal of Composites for Construction*. 2001. 5(4). Pp. 246–253.
18. Engindeniz, M., Kahn, L.F., Abdul-Hamid, Z. Repair and strengthening of reinforced concrete beam-column joints: State of the art. *ACI Structural Journal*. 2005. 102(2). Pp. 1. 187–197
19. Fujikura, S., Bruneau, M. Experimental investigation of seismically resistant bridge piers under blast loading. *Journal of Bridge Engineering*. 2011. 16(1). Pp. 63–71.
20. Hanoon, A., Kharnoob, M. Push-Out Test of Steel-Concrete-Steel Composite Section for Pre-Installation and Post-Installation Techniques of Shear Connectors. *Key Engineering Materials*. 2020. 862. Pp. 12–16. DOI: 10.4028/www.scientific.net/KEM.862.12
21. Kharnoob, M.M., Hasan, A.J., Sabti, L.M. The Limitation and Application of geometric Buildings and Civil Structures. *E3S Web of Conferences*. 2021. 318(4). 04009. DOI: 10.1051/e3sconf/202131804009
22. Al-Ansari, A.A., Kharnoob, M.M., Kadhim, M.A. Abaqus Simulation of the Fire's Impact on Reinforced Concrete Bubble Deck Slabs. *E3S Web of Conferences*. 2023. 427(10). 02001. DOI: 10.1051/e3sconf/202342702001
23. Abbood, A.A., Kharnoob, M.M. Experimental Studies on the Fire Flame Behavior of Reinforced Concrete Beams with Construction Joints. *E3S Web of Conferences*. 2023. 427(1). 02018. DOI: 10.1051/e3sconf/202342702018
24. Kharnoob, M.M., Cepeda, L.C., Jácome, E., Choto, S., Alazbjee, A.A., Sapaev, I.B., Hussein, M.A.M., Yacin, Y., Alawadi, A.H.R., Alsalamy, A. Analysis of thermoelastic damping in a microbeam following a modified strain gradient theory and the Moore-Gibson-Thompson heat equation. *Mechanics of Time-Dependent Materials*. 2023. DOI: 10.1007/s11043-023-09632-w
25. Kharnoob, M.M., Hasan, F.F., Sharma, M.K., Zearah, S.A., Alsalamy, A., Alawadi, A.H.R., Thabit, D. Dynamics of spinning axially graded porous nanoscale beams with rectangular cross-section incorporating rotary inertia effects. *Journal of Vibration and Control*. 2023. DOI: 10.1177/10775463231222531
26. Klyuev, S.V., Kashapov, N.F., Radaykin, O.V., Sabitov, L.S., Klyuev, A.V., Shchekina, N.A. Reliability coefficient for fibreconcrete material. *Construction Materials and Products*. 2022. 5(2). Pp. 51–58. DOI: 10.58224/2618-7183-2022-5-2-51-58
27. Strelkov, Yu.M., Sabitov, L.S., Klyuev, S.V., Klyuev, A.V., Radaykin, O.V., Tokareva, L.A. Technological features of the construction of a demountable foundation for tower structures. *Construction Materials and Products*. 2022. 5(3). Pp. 17–26. DOI: 10.58224/2618-7183-2022-5-3-17-26
28. Kashapov, R.N., Kashapov, N.F., Kashapov, L.N., Klyuev, S.V., Chebakova, V.Yu. Study of the plasma-electrolyte process for producing titanium oxide nanoparticles. *Construction Materials and Products*. 2022. 5(5). Pp. 70–79. <https://doi.org/10.58224/2618-7183-2022-5-5-70-79>
29. Kashapov, R.N., Kashapov, N.F., Kashapov, L.N., Klyuev, S.V. Plasma electrolyte production of titanium oxide powder. *Construction Materials and Products*. 2022. 5 (6). P. 75 – 84. DOI: 10.58224/2618-7183-2022-5-6-75-84
30. Hussein, O.H., Ibrahim, A.M., Abd, S.M., Najm, H.M., Shamim, S., Sabri, M.M.S. Hybrid Effect of Steel Bars and PAN Textile Reinforcement on Ductility of One-Way Slab Subjected to Bending. *Molecules*. 2022. 27. DOI: 10.3390/molecules27165208
31. Zeybek, Ö., Özkılıç, Y.O., Çelik, A.İ., Deifalla, A.F., Ahmad, M., Sabri, M.M. Performance evaluation of fiber-reinforced concrete produced with steel fibers extracted from waste tire. *Frontiers in Materials*. 2022. 9. DOI: 10.3389/fmats.2022.1057128

Information about authors:

Majid Kharnoob, PhD

ORCID: <https://orcid.org/0000-0001-5922-5122>

E-mail: dr.majidkharnoob@coeng.uobaghdad.edu.iq

Received 05.03.2023. Approved after reviewing 10.07.2023. Accepted 08.12.2023.